

Fully 3D Printed 2.4 GHz Bluetooth/Wi-Fi Antenna

Paul Deffenbaugh, Kenneth Church
The University of Texas El Paso
500 W. University Ave
El Paso, TX 79968, US
Ph.: 407-275-4720
Email: pdeffenbaugh@miners.utep.edu

Josh Goldfarb, Xudong Chen
nScript, Inc.
12151 Research Parkway, Suite 150
Orlando, FL 32826, US

Abstract

3D printing and printed electronics are combined to demonstrate the feasibility of printing electrically functional RF devices. A combined process is used to demonstrate the feasibility of fabricating a 2.4 GHz antenna in a fully-3D printed object. Both dielectric, which also serves as the structure, and conductors are printed. Full-wave models are generated using Ansoft HFSS. Real-world tests using a Class 1 “100 m” Bluetooth module are conducted and compared against the performance of an industry-standard quarter wavelength monopole antenna.

Key words

3D Printing, Additive Manufacturing, Antenna, Direct Printing.

I. Introduction

3D printing is mature for fabricating complex 3D structures and this is currently done using varied materials such as polymers and metals. Heterogeneous 3D printing is more challenging given the issues of adhesion and thermal mismatch. Melding diverse materials for enhanced mechanical properties is common and exploited in the area of composites. Electronics are made with diverse materials but are not typically made with structure as the focus, but instead electrical function. FR4 is a standard composite used for Printed Circuit Boards (PCB). PCBs have the advantage of combining a number of diverse electronic components and including antennas. Another approach for antenna fabrication is to print on flexible but flat substrates and place the antenna within a structure.

Currently wireless smart objects are simply objects which have electronic circuit modules and antennas placed inside them. Much work has been done in the area of thin film RFID antennas and circuits however these devices are still placed into objects [1] [2]. Thin film antennas are flexible and may be easily adhered to objects but this requires extra processing steps to fabricate the antenna and apply it to the target object. Work has been done in larger printed antennas however the

extra processing step of electro-less plating is used to metallize all surfaces [3]. Little work has been done in the area of 3D printed antennas in 3D printed objects, an opportunity that eliminates the need to separately fabricate and install electronics in objects thus reducing processing steps.

Combining mechanical and electrical properties and forming a unique 3D electrically structural device has merit but conventional fabrication methods are not conducive for this. One approach to do this is to combine 3D printing and printed electronic processes. Researchers have done a variety of demonstrative 3D printed electrical functional devices but the majority of these have been for DC applications [1] [4] [5]. A study and demonstration that integrates both mechanical structure and wireless functionality directly into an object is shown.

This paper presents a simple and efficient 2.4 GHz antenna in a 3D printed object. Full-wave models are generated using Ansoft HFSS. In order to demonstrate functionality real-world tests using a Class 1 “100 m” Bluetooth module are conducted and compared against the performance of an industry-standard quarter wave antenna.

Radiation pattern, resistive loss efficiency, effective

aperture, and matching are modelled, measured and compared. Antenna size is not considered since 3D printed antennas are able to use a large part of the object in which they are functioning as a substrate and are not confined to a PCB (such as with typical PCB trace or chip antennas) and do not protrude from the device (such as with “rubber-duck” antennas”). It should be noted however that the antenna presented here is of approximately the same size as a conventional quarter wave antenna.

In order to complete the project a simple remote temperature sensor is demonstrated and future work where all components are fabricated into the 3D printed structure is outlined.

II. 3D Printing and Printed Electronics

The original term for 3D printing is Additive Manufacturing (AM). AM is a layer by layer approach to fabricating 3D objects. This is a direct digital approach and therefore it is possible to fabricate complex structures that are not possible using other fabrication processes [6] [7]. Some AM processes use a two print process which implies a sacrificial material that is soluble in a specified solution and including water. A 3D object is designed using Computer Aided Design (CAD) software and this 3D image is then sliced into many layers that range from 100 microns in thickness to hundreds of microns in thickness. Each of these layers are then printed and layered. Experts over the years have optimized the union of layers to create a process that is repeatable and reliable. Common 3D printing processes are Fused Deposition Modeling (FDM), Stereolithography Apparatus (SLA), Ultrasonic Additive Manufacturing (UAM), Ink Jetting [8], and Direct Print Additive Manufacturing (DPAM) [9].

Printed electronics has a variety of processes used to obtain electronic function on thin substrates such as paper or plastic. These thin substrates are electrically compatible and are very similar in nature to standard paper used in magazines or newspapers which are processed using a roll to roll process. A significant portion of the printed electronics processes is done using the roll to roll approach. For non-roll to roll printed devices, these are sometimes referred to as Direct Writing (DW) [10]. DW is an implied slow process and therefore another term of Direct Print (DP) is used to express digital printing patterns and including DW processes but done so using multiple nozzles or increased speeds [9].

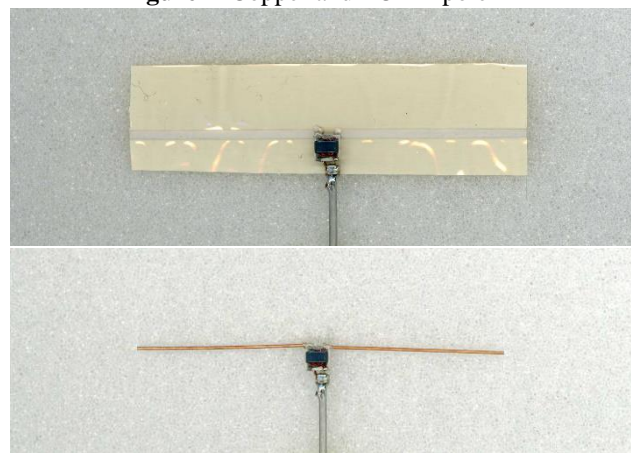
The combination of 3D printing and printed electronics is not a difficult concept to grasp since both of these are CAD processes. In addition to being CAD processes, there are also some closely related specific processes within these two broader areas. FDM and direct printing are both extrusion technologies and therefore it is feasible to put these on a common platform; this is what nScript has done with their 3Dn series. nScript has patented technology in micro-

dispensing for high viscosity applications such as silver paste and in addition also has technology in fused deposition that is similar to FDM which allows for finer features to be achieved; these share the same platform thus promoting the integration of 3D building and electronic integration.

III. Printed RF Antenna on Liquid Crystal Polymer (LCP) Substrate

A study and comparison of conductors on LCP vs. solid copper conductors, copper wire and printed dipoles are done at frequencies of 1.35GHz and 2.3GHz. It is expected the radiation pattern will reduce, thus reducing the gain of the antenna if the conductivity is not comparable or if the surface roughness is too great. If the cross sectional area of the printed line is not consistent over the length of the dipole, this can also affect the gain. The printed antenna and the copper dipole are shown in figure 1.

Figure 1 Copper and LCP Dipole



Models show the theoretical gain of a resonant half-wave dipole to be 2.2dBi. There will be additional losses in the balun transformer and in the antenna conductors. Both the copper wire and the printed antenna are lower than models due to the additional losses. Comparing the measured results of the antennas to each other demonstrated a consistent and near equal output.

Anechoic chamber measurements are taken for both antennas; the results are summarized in table 1 below. Test data shows good antenna gain and pattern, indicating that the performance of the printed antenna is similar to the copper wire device.

Table 1 Comparison of RF Characteristics

Antenna	Measured Gain [dBi]
Copper Wire 1.35GHz	1.97
LCP 1.35GHz	1.84
Copper Wire 2.3GHz	0.92
LCP 2.3GHz	0.96

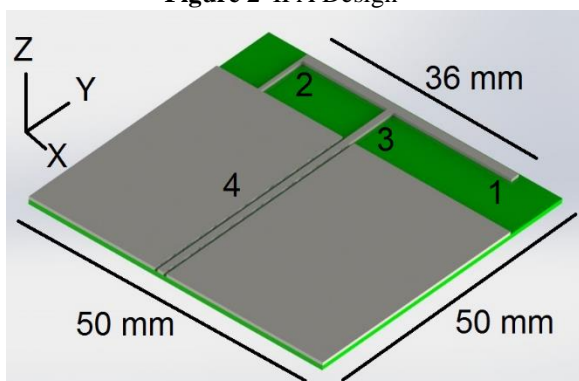
There is still more work to be done, but these results demonstrate the feasibility of the printed antenna approach.

IV. Antenna Design for Bluetooth

Several antenna designs are considered. Patch antennas may benefit greatly from 3D printing because of the flexibility over thickness that is offered when a structure is printed as opposed to etched into copper-clad circuit board material. Patch antenna properties are improved with increased dielectric height but feed lines require thin boards. 3D printing frees the designer to vary the dielectric thickness as needed. However patch antennas are highly directional and narrow-band, properties not desirable for objects which are typically used in random orientations and with frequency-hopping spread-spectrum (FHSS). Meander-line antennas are commonly used for their compactness. 3D printing offers the chance to take the antenna off the PCB and integrate the antenna into the case or structure thus freeing the antenna designer from cramped circuit board areas while allowing increased antenna efficiency with larger designs. Monopole and dipole antennas may be excellent choices however these types typically require a lumped-element balun and may have unacceptably-large nulls.

An inverted “F” antenna (IFA) design is chosen for its ease of matching, omni-directionality, and efficiency. These antennas are used commonly in cell phones for GSM, 3G, Wi-Fi, Bluetooth, and GPS. IFAs have four main components. 1) A radiating element, 2) an L-shaped inductor, 3) a short feed line, and 4) a ground plane split by a coplanar waveguide. Figure 2 illustrates the antenna structure, basic dimensions, chosen axis orientation, and the four main components by number.

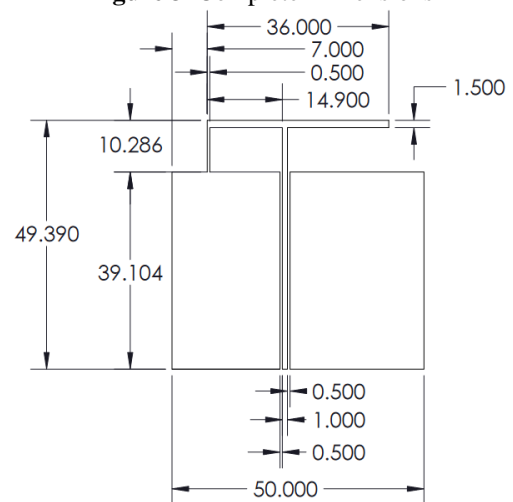
Figure 2 IFA Design



Complete antenna dimensions are shown in figure 3 and are chosen as follows. The length of the radiating element is one quarter wavelength at 2.45 GHz and tuned to 36 mm. An inductor (the “top” of the “F”) is formed by a 7 mm length of 0.5 mm width line and aids in matching. The radiating element is fed at a position which is calculated as the length divided by 3.5 [12]. The 50 ohm coplanar waveguide feed is

has a width of 1 mm and spacing of 0.5 mm on a 0.8 mm board. The substrate is reasonably-sized considering the size of the antenna while making the ground area as large as possible, 50 x 50 mm. The ground plane measures 50 mm x 39.1 mm. The 3D-printable thermoplastic acrylonitrile butadiene styrene (ABS) is chosen because it is low-cost, easy to print, and readily-available in almost all 3D printing systems. It has the properties dielectric constant $\epsilon_r = 2.8$ and loss tangent $D = 0.003$ [11]. The ABS substrate is printed using a Stratasys Dimension 1200es low-cost 3D printer. Future dielectrics will be printed in the same machine as the conductor using nScript nFD systems which will reduce the process steps and allow for fully-integrated conductor and dielectric.

Figure 3 Complete Dimensions



V. Modeling

ANSYS HFSS v15.0.3 (8/5/2013) is used to model and simulate the antennas expected performance. Referring to Figure 4, the solid blue line shows measured data, the dashed green line shows HFSS data based on printed dimensions, and the red dotted line shows HFSS data based on design dimensions. Certain dimensions such as the CPW feed width and spacing as well as radiating arm width and length were slightly different from the design. These errors will be accounted for in future prints of this antenna.

The difference between the measured and HFSS model data (solid blue/dashed green, 1-2 dB) can be accounted for in the SMA to U.FL cable and U.FL surface-mount connector and conductive epoxy connection which were not accounted for in the model.

The ideal design shows better than 1.4:1 SWR from 2.4 – 2.5 GHz and a better than 2:1 SWR is achieved from 2.32 – 2.58 GHz. Referring to figure 5, the -10 dB bandwidth is 14.4 %.

Figure 4 SWR

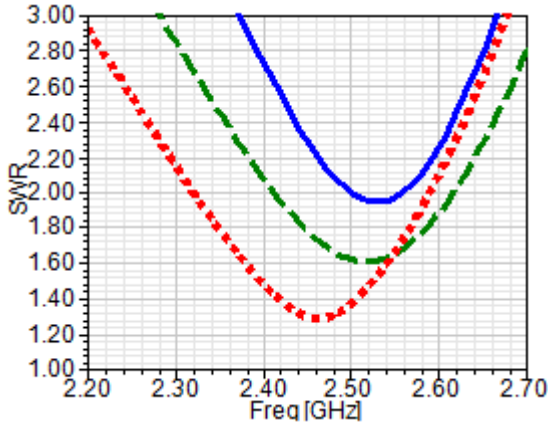


Figure 5 Return Loss

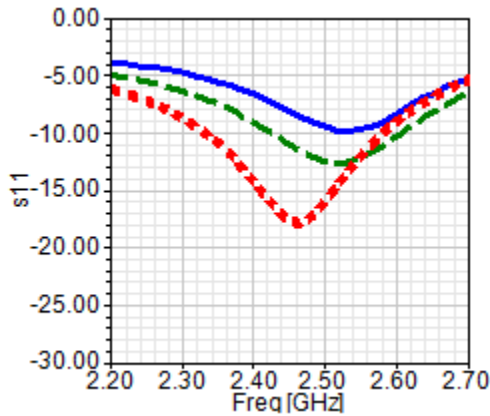


Figure 6 Reflection

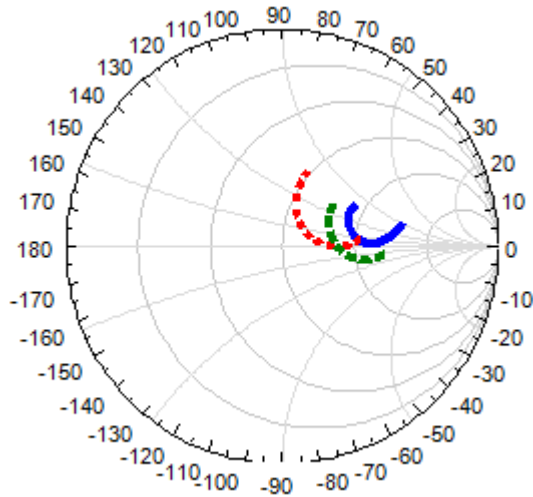
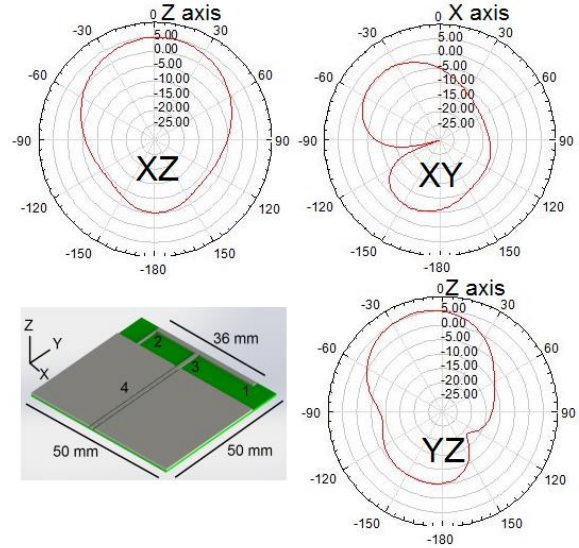


Figure 7 shows modeled radiation patterns. The maximum gain is 5.6 dB in the direction of the Z-axis up from the substrate plane. The gain is better than -10 dB in most directions with an expected null in the direction of the feed line and ground plane. See figure 7.

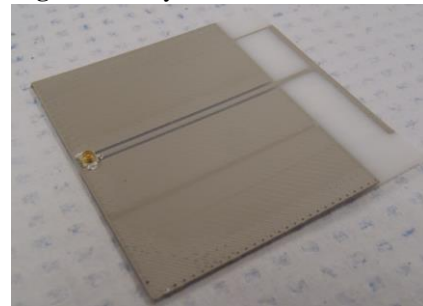
Figure 7 Radiation Patterns



VI. Structural Dielectric Fabrication

The substrate is formed using fused deposition modeling (FDM or FD). This 3D printing technology forms strong, low-loss dielectrics in a spatially arbitrary manner. Future antennas will take advantage of this opportunity to move away from planer into fully-3D integrated forms. For this design the print is flat, see figure 8.

Figure 8 Fully-3D Printed Antenna



FDM begins with a 3-D computer model in the STL file format. STL files contain a collection of triangles in a 3-D Cartesian coordinate system. These triangles are used to create the digital representation of the object. The STL file is then passed to a slicer which breaks the STL file into horizontal layers and then breaks down each layer into a collection of paths. It will typically output the paths as G-code instructions (the standard for computer numerical control (CNC)) that the printer will follow to construct the object. The first paths the slicer creates are outlines of the object. These perimeter lines serve as the shell of the object. The perimeters are then filled in with additional plastic. These lines are known as infill and serve to make the object solid. The density of the infill is not always 100% as significant amounts of time and plastic may be saved by making the object partially hollow. In fact objects are commonly printed with only 20% to 40% infill as greater densities offer diminishing returns in respect to additional

strength. The antenna printed here is printed 100% solid due to the thinness of the part however lower infill densities does offer the possibility of reducing material loss in larger microwave parts.

The printer constructs the object by extruding plastic while following the paths that the slicer calculated. The extrusion process starts at the filament feeding mechanism, referred to as a tractor feed. The tractor feed pushes the filament down a tube with an inner diameter (I.D.) that is only slightly larger than the filament itself. Contained near the end of this tube is the melt chamber, with the print nozzle being at the end of the tube. Depending on the temperature at any given position the filament will exist in one of three states; solid, liquid, or a soft state. The glass transition temperature (T_g) the filament is the approximate point above which the filament becomes soft. Controlling the plastic in these two states is not difficult do to the rigidity of the solid filament, and the viscosity of the liquid plastic. However, when the plastic is above the glass transition point but below the melting point, it will exist in a soft state and gain viscoelastic properties causing the plastic to behave similar to a rubber. As it has no rigidity, when downward pressure is applied to the filament it swells outward putting pressure onto the tube perpendicular to the intended direction of travel. This greatly increases the force needed to extrude the plastic. If the force becomes too great, the filament can slip or be ground away in the tractor feed. This results in either insufficient plastic deposition or no plastic flow at all. There are two solutions two this problem. Decreasing the coefficient of friction in the tube allows the plastic to be pushed downwards despite the side pressure. Second, by creating an extremely sharp transition from room temperature to the melt temperature, the height of the viscoelastic section of the filament is reduced to a negligible amount. After the plastic has passed into the liquid state, it is extruded through a small hole in the print nozzle, in the range of 300 to 600 μm . The part used in the 2.4 GHz antenna is fabricated using a 350 μm nozzle.

As the object is built up layer by layer the objects temperature becomes a gradient dependent on time and height. This can cause significant problems as each layer will contract at differing rates depending on their height. This causes the object to warp upwards as the lower layers cool and contract sooner than the layers above them. This can be solved in two ways. Ensuring a high adhesion rate between the first layer and the substrate can prevent the bottom layers from contracting at all thus minimizing the warping effect. However, the high internal stress within the object can cause the object to delaminate and split apart. The other method is by maintaining a build envelope temperature that is at the glass transition point. This allows all the layers to cool and contract together. Just as the object becoming too cold during a print can cause problems, so can keeping the object staying too hot. If the plastic is being laid too quickly, the heat can

build up in that area. This causes a severe degradation in print quality in the affected area.

There are some limitations in the geometry of the objects being printed unless a support material is used. For example, in order for overhangs to be printed successfully without support, they must not exceed a certain angle θ otherwise the lines of plastic will not be properly supported and will droop. This maximum overhang angle may be calculated using Equation 1 [13]. The variable w represents the printed width of the line which is approximately the same as the inner diameter of the nozzle and t represents the layer thickness.

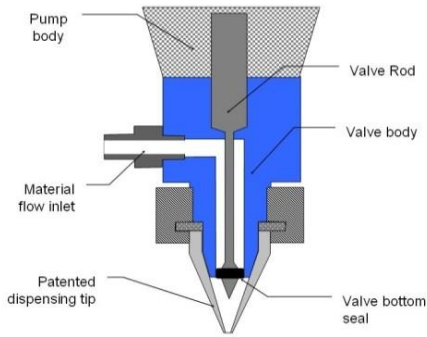
$$\theta = \text{atan}\left(0.5 \frac{w}{t}\right) \quad (1)$$

In our experience, the w/t ratio should normally be between 2 and 3 and a minimum of 1.25. Using a 350 μm nozzle (350 μm widths) this leads to layer thicknesses around 200 – 300 μm and maximum angles in the range of 36-52 degrees. The common design rule is 45° maximum angle. There is an exception to the width and thickness rule. If the angle of the overhang is equal to 0° (a “full” overhang) and is being supported on two or more sides the overhang may be printed if special care is taken during slicing. The slicer must ensure that the paths are routed such that all unsupported lines start and end at a location where there is plastic on the previous layer. If these conditions are met, the plastic is able to be strung through the air from one side to the next in much the same manner as power lines are strung between poles. Techniques such as these can be used to fabricate highly complex electromagnetic structures which would not be possible with planar manufacturing, would violate the rules of injection molding, or would require too much time using manual methods [6] [7].

VII. Conductor Fabrication

Material patterning onto the printed substrate or object in a controlled manner can be done using a variety of approaches. Micro dispensing is typically done using positive pressure on the material, which is transferred through a small orifice directly onto the desired surface. nScript micro dispensing technology uses a patented valve near the dispensing orifice to control the start and stop of the material flow. Traditional dispensing, including micro dispensing, is slow and lacks resolution and accuracy. However, nScript’s SmartPump™ technology controls the material volume flow at a pico-liter level, and the platform allows printing at high speeds. In addition, the valve enables clean starts and stops of the dispensing/ printing path. Figure 9 shows a view of the cross section of the valve assembly.

Figure 9 nScript SmartPump™ valve assembly.



The valve rod is driven by a motor and travels up and down in the channel of the valve body with a resolution of 0.1 μm . The shape of the patented pen tip is specially designed to reduce the pressure needed to push material through the orifice compared to the commonly used tubular needle, enabling dispensing through very small holes, such as 100 μm or less. This assembly is capable of handling materials with very high viscosities and also loaded particles. The material is typically transferred from a syringe or a customized cartridge by a positive pressure through the material flow inlet into the valve. The removable print head assembly is easy to take off when changing the material or cleaning. The additional benefits of nScript SmartPump™ include a reduction in material waste because there is only a fraction of a milliliter dead volume in the entire pump/valve setup.

When dispensing is initialized, the valve opens, which allows the material to flow through the pen tip onto the substrate. To stop the dispensing, the valve rod moves to a closed position that not only keeps a seal to the channel, but also maintains a negative pressure in the dispensing tip chamber to induce a reverse of the material flow [14]. The valve will open and close in a synchronized manner with the X and Y motion control. This allows any pattern to be printed in an X, Y plane and, if necessary, conformally in the Z plane. The linear print speed of X and Y can be as fast as 500mm/second on a gantry system, and the resolution and repeatability of motion in all directions is within a few micrometers. In addition to the SmartPump™ and the motion platform, a high resolution vision/camera system is also integrated for substrate alignment and a real-time processing view.

The printing pattern can be generated by a number of CAD software packages. The output of the CAD is transferred into a script file using nScript software; this provides integrated, synchronous commands for the machine. There is no need for a screen mask or other complicated setup in the process, in this digital manufacturing approach, which enables rapid prototyping. Also, higher speeds enable rapid manufacturing. This combination can reduce cost and maintenance on the production floor. In addition, the maskless approach allows for a variety of patterns printed digitally, the precision of the XYZ motion allows for conformal printing, and the ability to dispense a wide range

of materials promotes the potential to print in 3D or implement high aspect ratio features.

The IFA is printed on ABS dielectric and is shown in figure 8. There are a number of critical attributes, but some of those include line width, of the center strip as well as the gap between the center strip and the ground planes. An inductive line is printed from the antenna to one of the ground planes and this has critical dimensional features also. The advantage of the given control as mentioned earlier promotes the necessary features to obtain a working device.

Dupont CB-028 silver flake ink is deposited onto the surface of the FDM substrate using an nScript SmartPump™ and 3Dn-450 direct printing machine. Designs are loaded in the DXF file format and the printing parameters are shown in table 2.

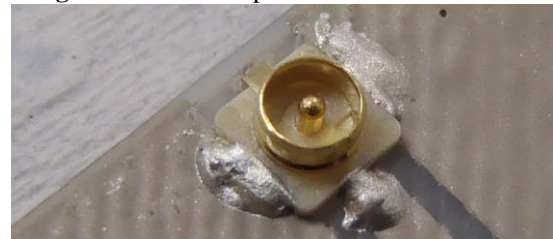
Table 2

Tip	125/175 i.d./o.d. (μm)
Line width	200 μm
Dispense gap	100 μm
Speed	30 mm/s
Valving	0.5 mm at 8 mm/s
Pressure	8 psi

Ink drying is performed near the glass transition (maximum) temperature of ABS at 90 °C for 60 minutes in order to maximize the silver ink conductivity without damaging the substrate.

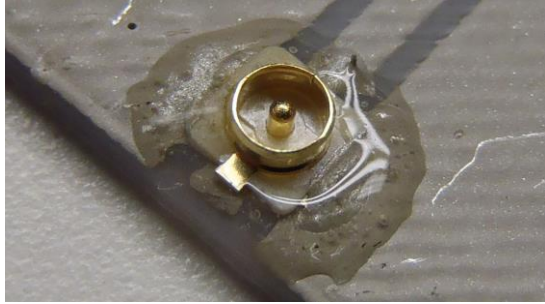
Surface-mount Hirose U.FL (UMCC) microwave connectors (figure 10) are used because of their small size and prevalence of use in both laptop and cell phone Wi-Fi and Bluetooth modules including the Bluetooth modules used during testing. Two-part conductive epoxy (Epotek H20E) is deposited in the area of the connector and the connector is installed. The epoxy is cured at 90 °C for 60 minutes. Curing of this type of epoxy does not occur even after 120 minutes at 70 °C, thus at least 90 °C must be used.

Figure 10 Silver Epoxied U.FL Connector



On top of the conductive epoxy, two part adhesive epoxy is applied (figure 11) to strengthen the connector attachment. The entire connector application process is designed for automation in the future by using a SmartPump™ and nScript pick-and-place module thus allowing a completely automated build process.

Figure 11 Glued U.FL Connector



VIII. Testing

Basic return loss measurements are conducted and are shown as the solid blue lines in figures 4, 5, and 6. An Agilent 8720 VNA and SOLT calibration are used at the SMA cable end. A 100 mm SMA to U.FL adapter cable is used to connect the antenna to the VNA, Cascade Microtech WinCAL software is used to save the s-parameter data to a computer, and HFSS is used to plot the data alongside the model data.

Testing is also conducted using a standard Bluetooth modules from Roving Networks (model number RN41XVU-IRM). The modules output +16 dBm during transmit and receive down to -80 dBm and use FHSS/GFSK in the band 2.402 – 2.480 GHz. The module is paired with a laptop computer and connected to another laptop using an RS-232 serial cable (FTDI Chip TTL-232RG-VREG3V3-WE) and the outdoor line of sight range is checked. Performance is compared against SMA quarter wave monopole antennas which are similar to those used in many laptop computer screens. The antennas used are Pulse part number W1010 having 2 dBi gain and $SWR \leq 2.0$ in the range 2.4 – 2.5 GHz. The antennas are connected to the Bluetooth modules using 100 mm SMA to U.FL cables. Measurements are conducted at an altitude of 1.5 m above ground. Results are summarized in table 3.

Table 3

Conventional Quarter-Wave Antenna	114 m
3D Printed Inverted F-Antenna	107 m

IX. Conclusion

It is shown here that it is possible to 3D print antennas for wireless devices which perform comparably to typical wire antennas. Also, in the future it is possible to use integrated printing processes to fabricate entire devices using these same technologies. This opens the door for highly complex 3D printed wireless electronic devices. 3D printing allows microwave designers greater flexibility of design and increases in overall system performance.

Acknowledgment

The authors would like to acknowledge Ibrahim Nassar from the University of South Florida for his discussions of the

antenna modelling.

References

- [1] Dupont, "Processing Guide for Printing RFID Antennae," Dupont Microcircuit Materials, Available: http://www2.dupont.com/MCM/en_US/assets/downloads/prodinfo/R_FID_ProcessingGuide.pdf
- [2] A. Dziedzic, P. Slobodzian. "Modern Microelectronic Technologies in Fabrication of RFID Tags," Radioengineering Proceedings of Czech and Slovak Technical Universities, vol.20, no.1, April 2011 Available: http://www.radioeng.cz/fulltexts/2011/11_01_187_193.pdf
- [3] Y. Huang, et al., "Layer-by-layer stereolithography of three-dimensional antennas," Antennas and Propagation Society International Symposium, 2005 IEEE, vol.1A, no., pp. 276–279 Vol. 1A, Jul. 3, 2005.
- [4] S. Castillo et al., "Electronics integration in conformal substrates fabricated with additive layered manufacturing", Proceedings of the 20th Annual Solid Freeform Fabrication Symposium, 2009, University of Texas at Austin, Austin, TX, pp. 730-737.
- [5] C. D. Gutierrez, "Three-dimensional structural electronic integration for small satellite fabrication," M.S. thesis, Elect. Eng., Univ. of Texas at El Paso, El Paso, TX, 2012, Available: <http://digitalcommons.utep.edu/dissertations/AA11512575>
- [6] R. Rumpf and J. Pazos, "Synthesis of spatially variant lattices," Opt. Express, 15263-15274, 2012.
- [7] R. Rumpf, et al., "3D Printed Spatially Variant All-Dielectric Metamaterials," unpublished, Jan. 2013.
- [8] R. X. Rodriguez and K. Church, "Process Development for Micro-Electronics Packaging with Direct Printed Additive Manufacturing," W.M. Keck Center for 3D Innovation, University of Texas at El Paso, El Paso, TX.
- [9] X. Chen, et al., "High Speed Non-Contact Printing for Solar Cell Front Side Metallization," 36st IEEE PVSC, 2010.
- [10] P. C. Joshi, et al., "Direct Digital Additive Manufacturing Technologies: Path Towards Hybrid Integration," Materials Science and Technology Division, Oak Ridge National Laboratory, Oak Ridge, TN.
- [11] P. I. Deffenbaugh, R. C. Rumpf, K. H. Church, "Broadband Microwave Frequency Characterization of 3-D Printed Materials," IEEE Transactions on Components, Packaging and Manufacturing Technology, accepted for publication, available for early-access: <http://ieeexplore.ieee.org/stamp/stamp.jsp?tp=&arnumber=6574280&isnumber=5673025>
- [12] I. Rosu, "Small Antennas for High Frequencies," [Online]. Available: http://www.qsl.net/va3iul/Antenna/Small_Antennas_for_High_Frequencies/Small_Antennas_for_High_Frequencies.pdf
- [13] David (user name "orgemd"). (2012, Sept. 6). Curling overhang problems, [Online forum comment]. Message posted to: <https://groups.google.com/forum/#!msg/mendelmax/aLMH1cjbxrk/4YE5OvNmzj0J>
- [14] B. Li, et al., "Robust Printing and Dispensing Solutions with Three Sigma Volumetric Control for 21st Century Manufacturing and Packaging", MRS Spring 2007 Meeting, Symposium N: Printing Methods for Electronics, Photonics and Biomaterials, April 2007.